Nano Research 2015, 8(3): 774–789
DOI 10.1007/s12274-014-0560-6
Research Article

ISSN 1998-0124
CN 11-5974/O4

Structural analysis of a nanoparticle containing a lipid bilayer used for detergent-free extraction of membrane proteins

Mohammed Jamshad[1,§], Vinciane Grimard[2,§], Ilaria Idini[3,§], Tim J. Knowles[4,§], Miriam R. Dowle[5], Naomi Schofield[1], Pooja Sridhar[4], Yupin Lin[1], Rachael Finka[1], Mark Wheatley[1], Owen R. T. Thomas[6], Richard E. Palmer[5], Michael Overduin[4], Cédric Govaerts[2], Jean-Marie Ruysschaert[2], Karen J. Edler[3], and Tim R. Dafforn[1] (✉)

[1] *School of Biosciences, University of Birmingham, Edgbaston, Birmingham, B15 2TT, UK*
[2] *Université Libre de Bruxelles, SFMB - CP206/2, Bd. du Triomphe, Accès 2 1050, Bruxelles, Belgium*
[3] *Department of Chemistry, University of Bath, Claverton Down, Bath, BA2 7AY, UK*
[4] *School of Cancer Studies, University of Birmingham, Edgbaston, Birmingham, B15 2TT, UK*
[5] *Nanoscale Physics Research Laboratory and PSIBS, School of Physics and Astronomy, University of Birmingham, Edgbaston, Birmingham, B15 2TT, UK*
[6] *School of Chemical Engineering, University of Birmingham, Edgbaston, Birmingham, B15 2TT, UK*
§ *These authors contributed equally to the work.*

Received: 11 October 2013
Revised: 30 July 2014
Accepted: 11 August 2014

KEYWORDS

nanoparticles,
lipid,
polymer,
membrane proteins,
structure,
detergent

ABSTRACT

In the past few years there has been a growth in the use of nanoparticles for stabilizing lipid membranes that contain embedded proteins. These bionanoparticles provide a solution to the challenging problem of membrane protein isolation by maintaining a lipid bilayer essential to protein integrity and activity. We have previously described the use of an amphipathic polymer (poly(styrene-co-maleic acid), SMA) to produce discoidal nanoparticles with a lipid bilayer core containing the embedded protein. However the structure of the nanoparticle itself has not yet been determined. This leaves a major gap in understanding how the SMA stabilizes the encapsulated bilayer and how the bilayer relates physically and structurally to an unencapsulated lipid bilayer. In this paper we address this issue by describing the structure of the SMA lipid particle (SMALP) using data from small angle neutron scattering (SANS), electron microscopy (EM), attenuated total reflection Fourier transform infrared spectroscopy (ATR-FTIR), differential scanning calorimetry (DSC) and nuclear magnetic resonance spectroscopy (NMR). We show that the particle is disc shaped containing a polymer "bracelet" encircling the lipid bilayer. The structure and orientation of the individual components within the bilayer and polymer are determined showing that styrene moieties within SMA intercalate between the lipid acyl chains. The dimensions of the encapsulated bilayer are also determined and match those measured for a natural membrane. Taken together, the description of the structure of the SMALP forms the foundation for future development and applications of SMALPs in membrane protein production and analysis.

Address correspondence to t.r.dafforn@bham.ac.uk

1 Introduction

Membrane proteins make up approximately 40% of the proteome of most organisms, carrying out a range of diverse functions from catalysis to metabolite transport. This class of proteins also provides more than half of the therapeutic targets for modern drug discovery. However, only a modest number of high resolution structures of membrane proteins (as compared to water soluble proteins) have been deposited in the protein structure database. This lack of progress results from several technical challenges that occur during production and subsequent handling of membrane protein containing samples. As membrane proteins are embedded in a lipid membrane continuum, the first step of purification involves solubilisation of the individual proteins. This process generally requires the use of surfactants (i.e., detergents) that replace the lipids surrounding the membrane protein (for a review see [1,2]). However the surfactant:protein micelles that are formed do not adequately mimic the native membrane structure and typically lead to poor protein stability and potentially partial or full unfolding of the protein structure.

One strategy for overcoming the problem of membrane protein extraction has been to re-insert the membrane protein in a model lipid membrane, such as a proteo-liposome or disc-shaped lipid particles, such as bicelles and nanodiscs. These systems offer potential solutions but each suffers from significant issues. For example, bicelle formation requires very specific phospholipid compositions and tight control of the experimental conditions. These conditions are often not compatible with experimental processes and/or the native lipid conditions required for protein activity. A second, more successful method, relies on a particle containing a lipid core stabilized by an annulus of apolipoproteins or derived peptides (also called membrane scaffold proteins (MSPs)) that protect the exposed hydrophobic edges of lipid membranes [3, 4]. Sligar and colleagues have led the development of these systems and have established the molecular layout of the MSP discs using a range of methods including X-ray scattering, nuclear magnetic resonance spectroscopy (NMR), molecular dynamics simulations and atomic force microscopy (see [5] for a comprehensive review). This method has led the way in showing that discoidal encapsulation can provide pure preparations of a range of membrane proteins including cytochromes [6], 7TM proteins (including G-protein coupled receptors) [7] and blood clotting co-factors [8] with native-like activity. The observation that the MSP system produces active membrane proteins is a good indication that the lipid environment in the MSP has native-like biophysical characteristics. This observation has been backed up by calorimetric measurements which show that the phase transitions of the lipid bilayer in the MSP is only minimally perturbed compared to that of the bulk lipid [9].

The pioneering studies of the MSP system—while demonstrating that the nanoencapsulation approach to membrane protein extraction may be useful—have been limited by their reliance on peptides as the lipid-stabilizing entity. This complicates the use of a number of biophysical techniques like circular dichroism (CD), Fourier transform infrared (FTIR) spectroscopy and NMR for studying these proteins, as the signals from the stabilizing peptides can interfere with signals from the membrane protein. In addition preparation of the disc:peptide:membrane protein complex relies on the use of surfactants with the resulting removal of the native lipid environment which cannot easily be replaced.

In 2001 Tighe and Tonge showed that poly(styrene-co-maleic acid) (SMA) could be used to produce nanoparticles that contained a synthetic lipid bilayer [10]. In 2009 we demonstrated that membrane proteins could be isolated as a nanoparticle which also contains a lipid bilayer using a SMA polymer which contained a 2:1 molar ratio of styrene to maleic acid [11]. We showed that this method did not require any surfactant and was amenable to biophysical studies, providing significant advantages over other available methods [11]. The addition of this co-polymer of styrene and maleic acid to biological membrane initiates the spontaneous formation of uniform discs (styrene maleic acid lipid particles (SMALPs)), many of which contain membrane proteins.

Although we have shown that the method can be used to purify and study a number of different membrane proteins, a detailed molecular characterisation

of the structure of these particles is however still missing. Recent work by Watts and colleagues [12–14] have shown a preliminary analysis of similar particles produced using a 9.5 kDa SMA polymer with a styrene to maleic acid ratio of 3:1 in contrast to the 2:1 ratio used in our previous experiments. Their work suggests that these particles are structurally monodispersed and stabilized by ionic interactions between the head groups of the lipids and the SMA. They show that these discs can be used to solubilize a range of proteins including Complex IV from the inner membrane of mitochondria [14] and bacteriorhodopsin [13]. The analysis of the encapsulated bacteriorhodopsin agrees well with our own previously published work using SMALPs to encapsulate the same protein [11]. Watts and colleagues also show that the phase transitions of the lipids in the nanoparticle are perturbed with the phase transition temperature being reduced by 7 ˚C compared to that for an equivalent bulk bilayer [12], indicating that the 3:1 SMA can significantly alter the physical properties of the membrane.

Here we provide an in depth study of the structural and physical properties of SMALPs made using SMA with a 2:1 styrene to maleic acid ratio and the lipid 1,2-dimyristoyl-*sn*-glycero-3-phosphocholine (DMPC). The overall structure of the SMALP particle is assessed using small angle neutron scattering (SANS) combined with isotopic phase contrast and electron microscopy (EM). These data provide information on the dimensions of the particle and the position of the SMA polymer and lipids, confirming that the membrane dimensions match those in the natural bilayer. Polarized attenuated total reflection FTIR (ATR-FTIR) spectroscopy is used to examine the orientation of the chemical groups of the polymer in the particle and to provide some information about the lipid organization in the disc. The interaction between the styrene groups and the lipid acyl chains is also defined using NMR. Finally the effect of the SMALP formation on the lipid phase transitions is analysed using differential scanning calorimetry (DSC) showing that the formation of this particle perturbs the phase behavior to a lesser extent than the particles made using MSPs or with SMA containing 3:1 styrene: maleic acid ratio. Together this study provides a comprehensive understanding of how these nanoparticles preserve a natural membrane microenvironment as a minimal functional unit.

2 Experimental

2.1 Materials

Poly(styrene-co-maleic anhydride) with a ratio of 2:1 styrene to maleic anhydride was used as described in Knowles et al. [11]. DMPC, ^{2}H-DMPC and deuterated 1,2-dipalmitoyl-*sn*-glycero-3-phosphocholine (^{2}H-DPPC) were purchased from Avanti Polar Lipids (Alabaster, AL) as synthetic lipids in powder form. All other materials were purchased from Sigma Aldrich Ltd. (UK).

2.2 Preparation of styrene maleic copolymer

A 10% solution of styrene maleic acid copolymer was prepared by dissolving 25 g of styrene maleic anhydride copolymer in 250 mL of NaOH [1 M] in a round bottom flask on a magnetic stirrer overnight. The resulting solution was then refluxed for 2 h and allowed to cool to room temperature. The material was then aliquoted into 50 mL samples and placed in a freezer, and thawed and dialyzed against a buffer solution before use.

2.3 Preparation of styrene maleic acid lipid particles

For all experiments SMALPs were prepared by first preparing two solutions; the first solution was of 10% (wt/vol) of the required phospholipid prepared by suspending lipid powder in a known volume of phosphate buffer solution, then sonicating for ~5 min to disperse the lipid in the solution. A second solution consisting of 10% (wt/vol) copolymer in buffer was prepared as outlined above. The two solutions were then combined to give the desired concentrations, routinely this was 1% lipid and 2.5% SMA. This mixed solution was shaken for approximately 1 min until clear.

Where required, gel filtration purification of the initial disc suspensions was performed to remove any high molecular weight aggregates that might affect data collection. SMALPs were purified at 6 ˚C using a

Superdex 200 10/300 GL column attached to an AKTA™ purifier fast protein liquid chromatography (FPLC) purification system (GE Healthcare). A 50 mM phosphate buffer with 200 mM NaCl was used with a flow rate of 1 mL/min. Absorbance measurements were recorded at 254 nm.

2.4 Small angle neutron scattering

After gel filtration the SMALPs were dialysed sequentially into appropriate buffer solution (50 mM phosphate buffer with 200 mM NaCl, pH 8.0) in H_2O, D_2O or mixtures of H_2O/D_2O for SANS measurements. The SANS experiments were conducted on the D11 instrument located at the Institut Laue-Langevin (ILL) laboratories, Grenoble (France). Samples were measured in single stopper rectangular Hellma quartz cuvettes with a 1 mm path length. This instrument uses a monochromatic neutron beam with a wavelength of 6 Å and the detector was placed at 1.2 m, 7 m, and 13 m to collect a Q range between 0.004–0.5 $Å^{-1}$. Water was used as the calibration standard. Measurements were taken at 25 C. The experiment was performed using four different phosphate buffer contrasts, 100% H_2O, 100% D_2O, 60% D_2O, and 32% D_2O.

2.5 Transmission electron microscopy

The SMALP sample was diluted in buffer solution (50 mM sodium phosphate pH 7.0, 100 mM NaCl) to 1×10^{-5} mg/mL. The sample was then drop cast onto a glow discharged carbon coated electron microscopy grid and negatively stained with uranyl acetate. Imaging was performed with an FEI Tecnai 12, 120 kV transmission electron microscope (TEM) with an FEI Eagle 4k × 4K charge-coupled device (CCD) camera. All subsequent image processing was carried out using Fiji/ImageJ.

2.6 ATR-FTIR

ATR-FTIR spectra were recorded at room temperature with a Bruker EQUINOX 55 FTIR spectrophotometer equipped with a liquid nitrogen-cooled mercury cadmium telluride (MCT) detector at a nominal resolution of 2 cm^{-1}. The internal reflection element (IRE) was a diamond, with an incidence angle of 45° leading to one internal reflection. The spectrophotometer was continuously purged with air dried on a Hydrovane HV05.

A 1 μL sample was deposited on the diamond element and dried under a nitrogen stream. Spectra were recorded either in the absence of polarization of the light, or with the incident light polarized parallel and perpendicular to the diamond surface. Dichroic spectra were computed by subtracting the parallel polarized spectrum from the perpendicularly polarized spectrum. Correction for differences in evanescent field intensity for each polarization was done by normalizing the spectrum with respect to the area of the lipid ester band at 1,740 cm^{-1}, estimated to be equal in both directions [15]. An upward deviation in the dichroic spectrum indicates a dipole having preferentially a near-normal orientation with respect to the diamond surface, while a downwards deviation in the dichroic spectra indicates a dipole oriented in the plane of the diamond surface. Spectra were corrected, if necessary, for water vapor, using water vapor spectra recorded with the same polarization of the light.

2.7 NMR spectroscopy

Acyl-deuterated and non-deuterated DMPC SMALPs were prepared by adding 2.5% SMA in 50 mM sodium phosphate pH 8.0, 300 mM NaCl to a 2% (*w*/*v*) liposome suspension of either 1,2-dimyristoyl(d_{54})-*sn*-glycero-3-phosphocholine or 1,2-dimyristoyl-*sn*-glycero-3-phosphocholine in 50 mM sodium phosphate pH 8.0, 300 mM NaCl and incubating at room temperature for 10 min. The resultant SMALPs were purified by size exclusion chromatography using a Superdex 200 10/300 GL column (GE Healthcare) with a buffer consisting of 50 mM sodium phosphate, 200 mM NaCl pH 7.5.

A two-dimensional (2D) homonuclear nuclear overhauser effect spectroscopy (NOESY) experiment [16, 17] was obtained with a mixing time of 100 ms on a Varian Inova 800 MHz spectrometer equipped with 5 mm *z*-PFG cryogenic probe. Data were processed using NMRpipe [18] and spectra analysed using Sparky [19].

2.8 Differential scanning calorimetry

DMPC vesicles were prepared by solubilizing DMPC in chloroform and then drying under rotary evaporation

to produce a thin layer of lipid. The lipid was then resuspended in 50 mM TrisHCl pH 8.0, 200 mM NaCl to a final concentration of 2 mM. 0.1 μm unimolecular vesicles were produced by subjecting the hydrated lipid suspension to 10 freeze/thaw cycles followed by extruding through 0.1 μm pore size membranes above the phase transition temperature of the lipid (for DMPC > 25 ℃). DMPC SMALPs were prepared as described for NMR spectroscopy but concentrated down to a final lipid concentration of 6 mM.

A VP-DSC microcalorimeter (MicroCal, Northampton, MA) was used to carry out differential scanning calorimetry. Before making the scans, the samples were degassed for 20 min at 4 ℃. All samples were scanned from 5 to 95 ℃, at a scan rate of 70 ℃/h, with the prescan thermostat set for 15 min and the postscan thermostat 0 min. Thirty five scans were made for each sample in the high feedback mode with the post cycle thermostat set to 5 ℃.

3 Results

It has already been shown by ourselves and others [13] that SMALPs can provide a novel method for membrane protein extraction. However in order to progress the development of the method it is essential that an in-depth description of the structure of the particle itself is obtained. Such an understanding will enable future applications of the SMALP particle in studies of membrane proteins including pharmaceutical screening studies, structure determination and biochemical analyses. In addition a deeper understanding of the SMALP will provide baseline information for the continued development of new improved SMA based systems.

The study was begun by carrying out a detailed analysis of SMALPs using SANS data from SMALPs containing either hydrogenated or deuterated lipids. This provided information on the distribution of the polymer and the lipid components within the particle and data on the overall dimensions of the SMALP structure. TEM analysis of the SMALP provided more detail on the size distributions of the discs. Polarized FTIR spectroscopy experiments provided information on the orientation of the chemical moieties that make up the particle while NMR resolved interactions between the lipids and the polymer. In the last stage of the study calorimetric measurements showed that the phase transition temperature of the lipid bilayer remains very close to that of the free membrane. These data together provide a detailed picture of the structure of the SMALP that lays the foundation for further studies using the SMALP system to investigate protein structure.

3.1 Small angle neutron scattering

The first goal was to ascertain the shape and size of the SMALP and the positions of the lipid and SMA constituents within the nanoparticle. This architecture is important for supporting a native-like membrane structure for solubilization of biologically intact states. SANS offers the ability to examine the structure of materials like SMALPs free in solution, providing dimensions of the overall particle, while solutions containing varying amounts of D_2O as well as deuterated lipids could be used to determine the relative positions of the copolymer and lipids in the structure.

The data for four solution contrasts (100% H_2O, 100% D_2O, 60% D_2O, and 32% D_2O) were fitted simultaneously using the National Institute of Standards and Technology Small-Angle Neutron Scattering (NIST SANS) Analysis Package [20] in the IGOR Pro fitting program to a model of core–shell cylinders with a face layer on top and bottom to account for the phospholipid headgroups (a schematic representation is given in Fig. 1). The core radius was convoluted by a Schultz distribution to add polydispersity in the radius of the core of the particle. A Hayter–Penfold structure factor [21] for charged colloids in solution was used to account for electrostatic repulsion between the discs. The scattering length density (SLD) of the phospholipid headgroups was set to be 1.84×10^{-6} Å^{-2} based on the value cited by Smith et al. [22] who used molecular volumes obtained from molecular dynamics simulations to calculate this number. The water content of the headgroup layer was likewise set to a mole fraction of 0.57 based on their results in fitting a deuterated DMPC bilayer. The SLD of the polymer was calculated to be 1.81×10^{-6} Å^{-2} and the SLD of the rim fitted by fitting the mole fraction of solvent in the rim based on this value and that of the phosphate buffer solution for each sample.

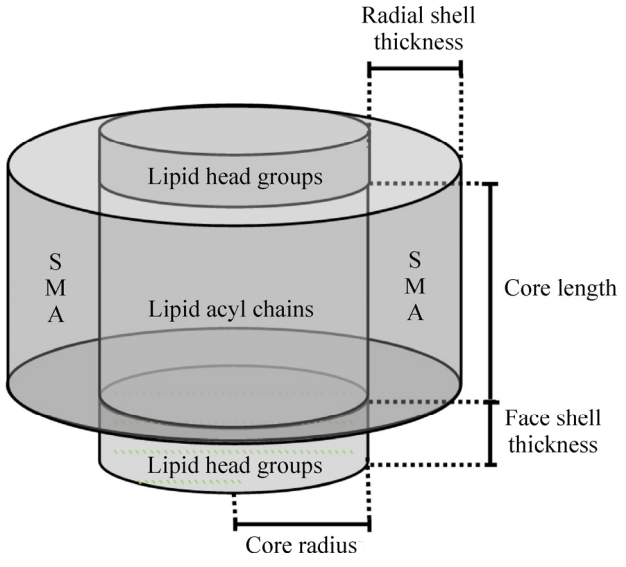

Figure 1 The core shell model used to fit the SANS data showing the dimensions that can be calculated from the model.

The scattering length densities of the 100% H_2O (-0.56×10^{-6} Å^{-2}) and 100% D_2O (6.3×10^{-6} Å^{-2}) buffer solutions were also calculated and held during fitting. Other model parameters which were predetermined and held constant during fitting were the temperature (298 K), the dielectric constant of the solution (78), and the monovalent salt concentration (250 mM based on the buffer preparation). The majority of other parameters were linked during fitting except for the SLDs of the two mixed H_2O/D_2O buffer solutions (to account for any incomplete exchange during dialysis), and the backgrounds for each sample. Fitting results are shown in Table 1 and the fitted data in Fig. 2.

These results show that the SMA polymer encircles a disc of lipid membrane with a radius of 38 ± 2 Å thus indicating an overall bilayer size of between 4,071 and 5,026 Å^2. These data also show that the bilayer in the SMALP is supported on the edges by a 7 ± 2 Å thick annulus of SMA indicating that the annulus is likely to be made up of a single thickness of the polymer.

The thickness of the core of the disc (which represents the lipid bilayer) of 26 ± 2 Å agrees well with the expected thickness of the hydrophobic region of a DMPC bilayer of 26.2 Å at 30 ℃ [23]. The thickness of the face layer, being measured as 8 ± 2 Å, which would be expected to represent the headgroups of the lipids also agrees well with previous measurements of 9 Å [23].

3.2 Transmission electron microscopy

TEM studies of the structure of the SMALP provide information on the gross morphology and dimensions of the particle. Images from TEM confirm the overall disc shaped nature of the SMALP (Fig. 3). The

Table 1 Fit parameters for fitting SANS data to a model of a charged core–shell cylinder with polydisperse core and headgroup regions at top and bottom of the cylinder

Model coefficients	100% D_2O	60% D_2O	32% D_2O	0% D_2O
Volume fraction	0.019 ± 0.01			
Mean core radius (Å)	38 ± 2			
Radial polydispersity (sigma)	0.35 ± 0.05			
Core length (Å)	26 ± 2 (26.2)			
Radial shell thickness (Å)	9 ± 2			
Face shell thickness (Å)	10 ± 2 (5.25)			
Calculated total bilayer thickness (Å) = core length + 2 × face shell thickness	46 (44)			
Core SLD (Å^{-2})	6.5×10^{-6} ± 0.05×10^{-6}			
Mol% solvent in face	0.57[a]			
Mol% solvent in rim	0.42 ± 0.05			
Solvent SLD (Å^{-2})	6.29×10^{-6} [a]	$3.86 \times 10^{-6} \pm 0.05 \times 10^{-6}$	$1.87 \times 10^{-6} \pm 0.05 \times 10^{-6}$	-0.57×10^{-6} [a]
Charge on the disc	0.31 ± 0.05			
Incoherent background (cm^{-1})	0.015 ± 0.05	0.011 ± 0.05	0.022 ± 0.05	0.006 ± 0.05

[a] Calculated or set from literature values and held during fitting. Figures in brackets are derived from the Ref. [8] for a DMPC bilayer at 30℃.

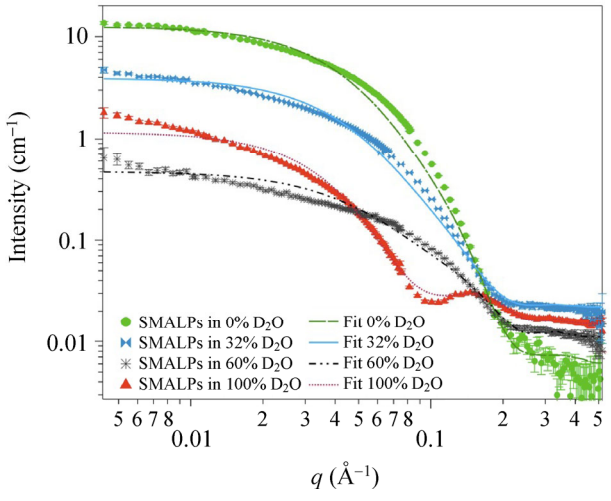

Figure 2 Scattering patterns from SMALPs fitted to the model described in the text. Dotted lines represent the experimental results while plain lines represent the fitting.

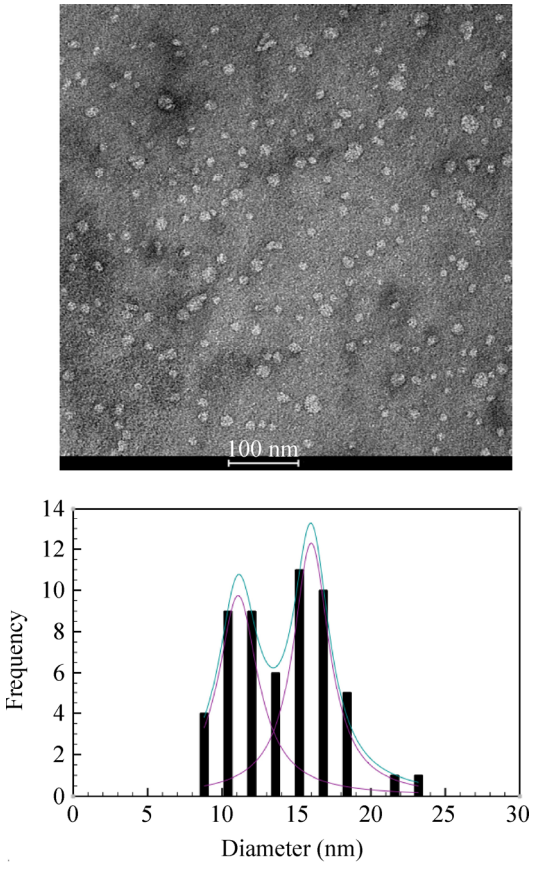

Figure 3 Top: Negative stain TEM image of SMALPs. Bottom: Histogram showing the distribution of the diameters of SMALP particles.

dimensions of these particles clearly show some variability. A measurement of the diameters of a population of SMALPs using TEM shows a bimodal distribution of diameters. Analysis of this distribution using a Gaussian distribution model shows the presence of two maxima at 11.1 ± 3.3 nm and 16.0 ± 3.0 nm. These dimensions are larger than those observed in the SANS experiments, which suggest a maximum diameter of 9.8 nm. It is likely that this disparity reflects the different preparation methods for the two samples, the SANS date being averaged in buffered solution while the TEM images are taken of individual particles on a dried sample stained with uranyl acetate.

3.3 Polarized ATR-FTIR spectroscopy

ATR-FTIR is a powerful tool to study biological samples, and in particular biological membranes. It allows a simultaneous study of the structure of the various biological and chemical components present in the system, and does not require the introduction of any probe, which could perturb the system's integrity. Furthermore, when using polarized incident light, information about the orientation of the various chemical moieties of a molecule with respect to each other can be obtained [24]. Here infrared spectroscopy was used to study the orientation of the chemical moieties of the polymer with respect to the lipids. Assignment of the various bands of the SMA spectrum (Fig. 4) is summarized in Table 2. Bands related to the styrene moiety were assigned on the basis of the polystyrene spectrum [25]. Bands related to the maleic acid moiety were assigned from the spectra of succinic acid and SMA both recorded at pH 8 and pH 1 (data not shown).

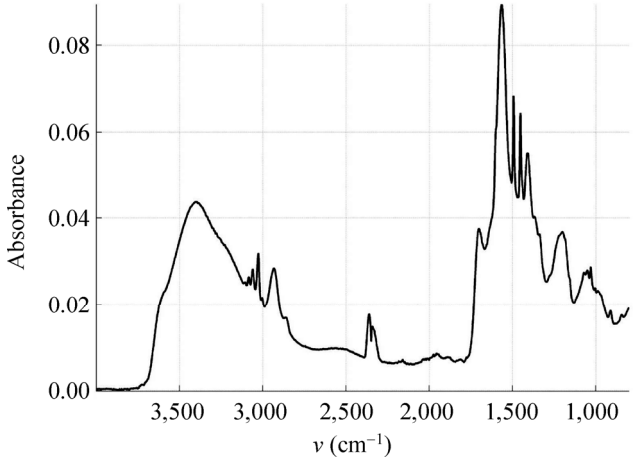

Figure 4 IR spectrum of SMA.

Table 2 Assignment of the bands of the SMA spectrum. Reference spectra were the spectra of polystyrene [25] and of succinic acid

Position (cm^{-1})		Functional group
SMA spectrum	Reference spectrum	
3083	3083	C–H stretching in the styrene ring (in *ortho* and *meta* positions of the substituted carbon)
3060	3061	C–H stretching in the styrene ring (in the *para* position of the substituted carbon)
3026	3029	C–H stretching in the styrene ring (in *ortho* and *meta* positions of the substituted carbon)
2932	2923	antisymmetric C–H stretching of the polymer backbone CH_2
2858	2851	symmetric C–H stretching of the polymer backbone CH_2
1705	1655	COOH stretching in maleic acid
1602	1602	ring vibration (C–C stretching)
1565	1550	COO^- stretching in maleic acid
1493	1493	ring vibration (C–C stretching)
1453	1450	C–H bending of the polymer backbone CH_2

Polarized spectra of the SMALPs were recorded using parallel and perpendicular polarized light. A dichroic spectrum was computed by subtracting the parallel polarized spectrum from the perpendicularly polarized spectrum after normalization, and comparisons with free polymer controls were made. Several bands show a positive deviation on the SMALP dichroic spectrum (Fig. 5). On the basis of the assignments made above, they correspond to the vibration of the styrene ring and to the COO^- stretching. As the COO^- transition dipole is parallel to the COO^- bisector and as the dipole of the styrene ring is in the plane of the ring, it means that the two polymer functions orient perpendicularly to the membrane plane. This suggests that the ring of the styrene intercalate between the lipid chains in a manner analogous to cholesterol. As a control, we did not detect any orientation of the free polymer deposited on the IR plate. The band corresponding to the C–H stretching of the polymer carbon backbone is not visible in the spectrum due to the overlap with the lipid C–H stretching bands of the lipid acyl chains. In order to detect C–H stretching of the polymer backbone, SMALPs were prepared with deuterated DMPC. In these conditions, C–D bands from the lipid acyl chains shifted to around 2,000 cm^{-1} and the C–H stretching bands of the polymer backbone at 2,858 and 2,932 cm^{-1} become visible (Fig. 6). The polarized infrared spectrum shows a positive deviation of the band at 2,932 cm^{-1}. As the dipole of the C–H bond is

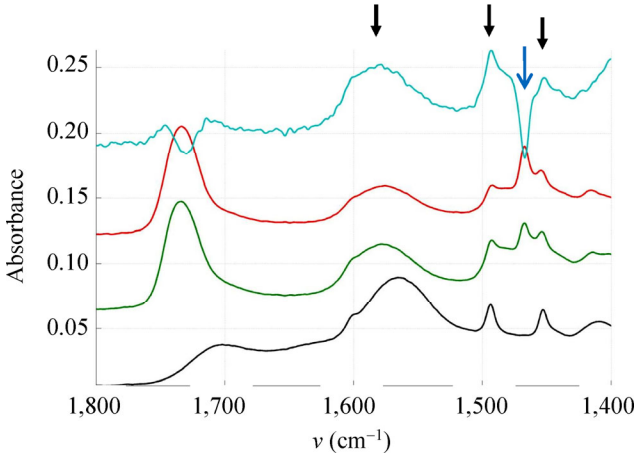

Figure 5 Dichroic spectrum of SMALPs. Black: Non-polarized spectrum of SMALPs (DMPC); Green/red: Polarized (0° and 90°) spectra of SMALPs; Blue: Dichroic spectrum of SMALPs. Black arrows show the positive deviation of SMA bands while the blue arrow shows the negative deviation of the lipid CH_2 bending band.

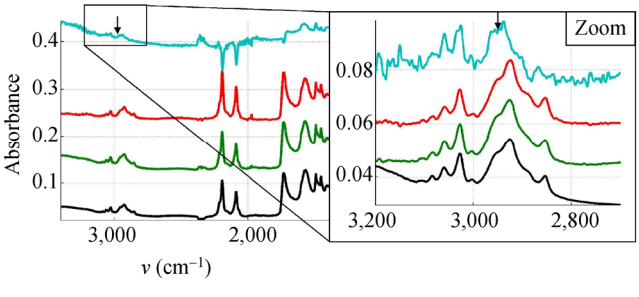

Figure 6 Dichroic spectrum of deuterated DPPC SMALPs. Black: Non-polarized spectrum of SMALPs (DMPC); Green/red: Polarized (0° and 90°) spectra of SMALPs; Blue: Dichroic spectrum of SMALPs. Arrows show the positive deviation of SMA bands.

perpendicular to the polymer backbone, it indicates an orientation perpendicular to the lipid acyl chain, compatible with the polymer forming a ring around the lipid in a manner that is analogous to the Apolipophorin III helices in High Density Lipoproteins (HDL)-like particles [26]. Interestingly, the COO^- band of the polymer is strongly shifted in the presence of lipids (to 1,575 cm^{-1} rather than 1,565 cm^{-1}) (Fig. 7), suggesting a specific interaction between the carboxyl function of the polymer and the lipid.

Lipid moieties present the typical signature of a bilayer organization, with a negative deviation in the dichroic spectrum for the symmetric and anti-symmetric stretching of the fatty acid CH_2 at 2,848 cm^{-1} and 2,915 cm^{-1} respectively (data not shown), as well as a negative orientation of the CH_2 bending band around 1,467 cm^{-1} (Fig. 5) and a positive orientation of the CH_2 wagging bands located between 1,200 and 1,330 cm^{-1} (Fig. 8) [26, 27]. However, small variations can be observed in comparison to the spectrum of pure DMPC. Upon interaction with SMALPs, the anti-symmetric and symmetric CH_2 stretching bands are shifted to higher wavenumbers, going respectively from 2,916.5 cm^{-1} to 2,918 cm^{-1}, and from 2,849 cm^{-1} to 2,850 cm^{-1} (Fig. 9). Such shifts have also been observed for lipids upon phase transition, and are representative of the C–C bonds shifting from *trans* conformation to *gauche* conformation. This suggests that the presence of the polymer may

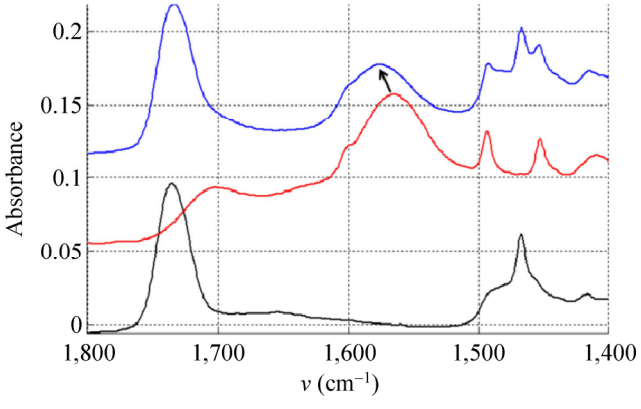

Figure 7 IR spectrum of SMALPs. Black: IR spectrum of DMPC; Red: IR spectrum of SMA; Blue: IR spectrum of DMPC SMALPs. The arrow shows the shift from 1,565 to 1,575 cm^{-1} of the maximum of the SMA band corresponding to the COO^- stretching.

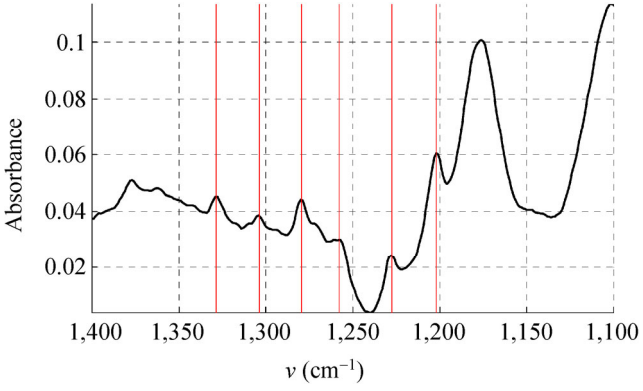

Figure 8 Dichroic spectrum of DMPC SMALPs. CH_2 wagging bands are indicated by red lines.

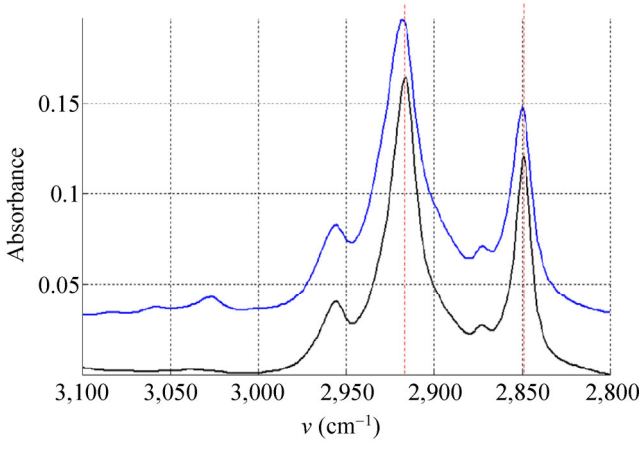

Figure 9 Shift of the C–H stretching bands in SMALPs. Black: IR spectrum of DMPC; Blue: IR spectrum of DMPC SMALPs. Red dashed lines have been added to better visualize the shift.

force some of the lipid aliphatic chains to kink, inducing the formation of a C–C bond in a *gauche* conformation. However a complete transition should induce a shift of about 3 cm^{-1} [28], indicating that only some of the aliphatic chains undergo this change of conformation. Similarly, the bands corresponding to the wagging of the C–H bonds of the aliphatic chain, that only appear when the aliphatic chain is in all-*trans* conformation, broaden and disappear when the temperature is increased due to the presence of bonds in the *gauche* conformation. In our spectra, bands located at 1,180 (hidden by the absorption of the ester bond itself), 1,203 and 1,231 cm^{-1} (Fig. 10) also decrease in intensity after interaction with the SMA polymer suggesting the appearance of bonds in *gauche* conformation [27]. The dichroic spectrum allows observation of an almost complete wagging series of six bands (normally $n/2$ wagging bands, where n = 14,

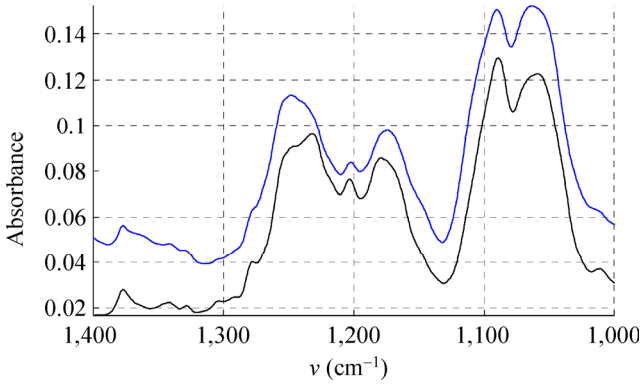

Figure 10 Decrease of the CH_2 wagging bands in SMALPs. Black: IR spectrum of DMPC; Blue: IR spectrum of DMPC SMALPs.

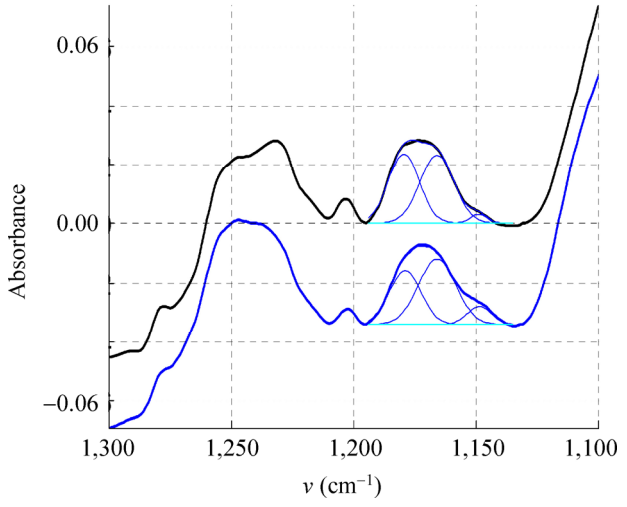

Figure 11 Deconvolution of the ester C–O stretching band. Black: IR spectrum of DMPC; Blue: IR spectrum of DMPC SMALPs. Dashed blue lines represent the fitting of the two components at 1,165 and 1,180 cm^{-1}.

the number of carbon atoms in the aliphatic chain of DMPC), with positive deviation at 1,202, 1,228, 1,258, 1,280, 1,304 and 1,328 cm^{-1} (Fig. 8). The dichroic ratio (i.e., the absorbance ratio of this band for spectra obtained with parallel and perpendicular polarized incident light) of the band at 1,202 cm^{-1} can be calculated. A dichroic ratio of 5.7 is obtained for the DMPC bilayer, and increases to 11.7 for the SMALP disc, which suggests a straightening or a decreased mobility of the lipid acyl chains in the bulk phase of the nanoparticle (as this only concerns the acyl chains that are in the all-*trans* conformation), potentially due to the constraint of the polymer scaffold. Similar behavior has previously been observed for lipids in HDL-like particles [29]. A decreased mobility of the lipids in SMALPs was also observed in a previous electron paramagnetic resonance (EPR) study [12]. Although the authors attributed it to a decrease in lipid-chain *gauche*–*trans* isomerization, a straightening of the acyl chains could also explain their results.

Further support for conformational constraints induced by the polymer can be deduced from the ester bond C–O stretching that absorbs either at 1,180 cm^{-1} (planar conformation), or at 1,165 cm^{-1} (*gauche* conformation). In a bilayer, the ester in the *sn*-1 position is planar, and the ester in the *sn*-2 position is *gauche*. Deconvolution of this peak into two components centered at 1,180 and 1,165 cm^{-1} respectively confirm this, as 48% is found in the planar conformation and 52% is found in the *gauche* conformation (Fig. 11). In contrast, in DMPC SMALPs, there is a decrease of the planar component to 41%, suggesting that some ester bonds may change slightly their conformation upon interaction with the polymer. Similar behavior has already been observed for lipids in HDL-like particles [29].

3.4 Nuclear magnetic resonance spectroscopy

The results from the scattering and infrared experiments suggest that the polymer is closely associated with the acyl chains of the lipids protecting them from the polar solvent. If this was the case it would be predicted that the styrene moieties on the SMA could pack into the hydrophobic interior of the bilayer, although other arrangements could be envisaged. To detect the interactions a 2D NOESY experiment was performed (Fig. 12). This experiment shows through-space interactions between nuclei within a distance of 5 Å. Examination of the 1D spectrum for SMA shows that the peak for styrene is broad indicating that the moiety exists in a number of environments. This could be explained in a number of ways. Firstly the polymer is known to exist in a number of complex conformations in solution, e.g. monodispersed or micellar aggregates, meaning that the styrenes can exist in a number of environments. Secondly, since the chemical context for the styrenes in the polymer chain is variant, the polymer is expected to have an alternating $(SM)_n$ followed by a $(SS)_n$ region providing two environments for the styrene. This is likely to be

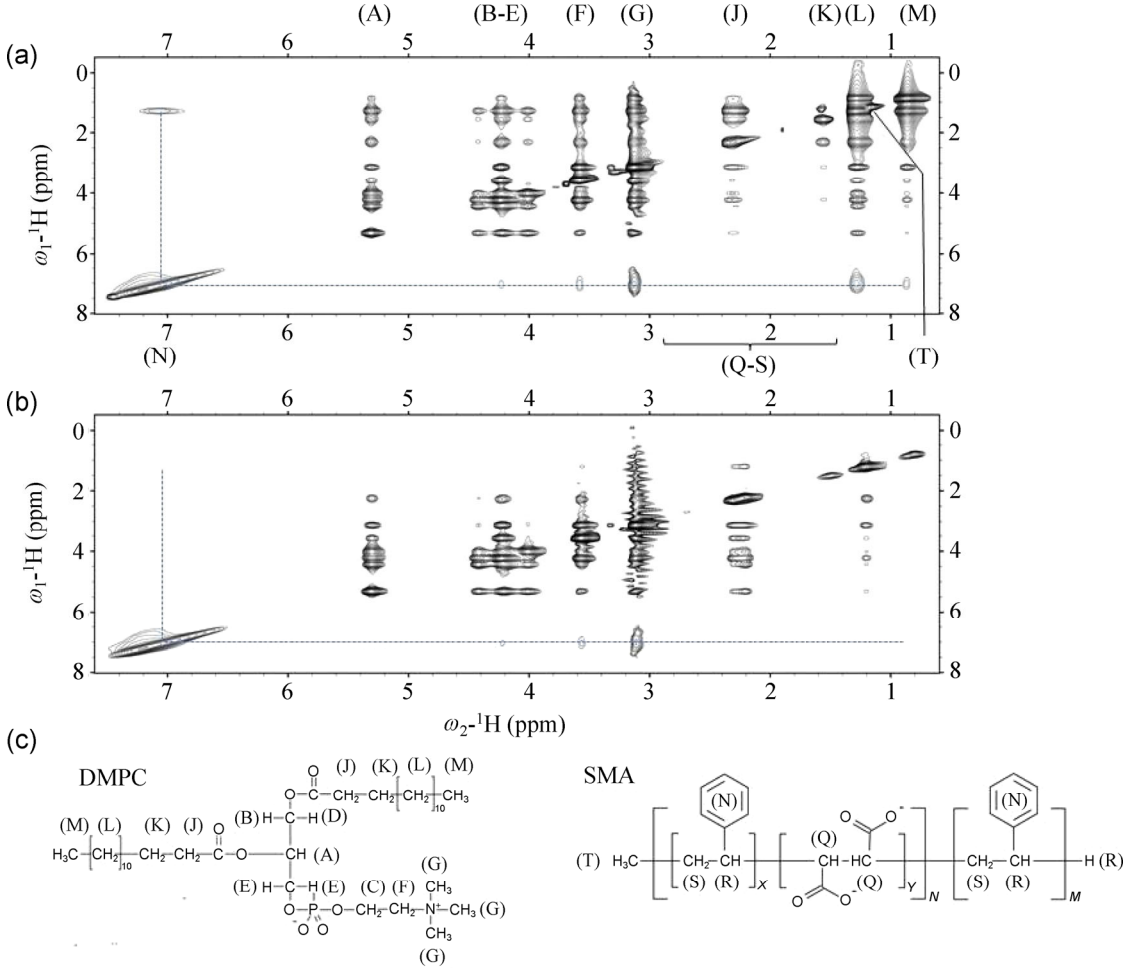

Figure 12 The SMA styrene groups in SMALPs show close proximity to the acyl chains of DMPC. (a) Homonuclear 2D dpfgse-NOESY of DMPC-SMALP in 50 mM sodium phosphate, 200 mM NaCl, pH 7 showing NOE interactions (dotted line) between the styrene group of SMA and DMPC. Signals for SMA groups Q–S are not observed due to the broadness of signal. (b) As in (a) but using 1,2-dimyristoyl-d54-*sn*-glycero-3-phosphocholine. The absence of NOEs at positions L and M confirm the predominant NOEs observed in (a) are to the acyl chain CH_2 groups and, to a lesser extent, the terminal CH_3 of DMPC. (c) Schematic representation of SMA and DMPC with groups labeled according to (a).

further varied by small regions of microvariation where the strict alternation is disrupted. Thirdly there is likely to be some dynamics and variation in the precise interactions between each of these species and the lipid bilayer. However despite this variation it is still possible to use NMR to determine the range of interactions between the lipid bilayer and the polymer. For DMPC-SMALP an intense nuclear overhauser effects (NOEs) was evident between the styrene of SMA and the acyl chain of DMPC (Positions L & M), thus confirming that the styrene group is positioned closely to the DMPC acyl chains. The NMR assignments of the acyl group were confirmed by comparing acyl deuterated DMPC, which abolished all NOEs from the styrene to DMPC proton positions L and M, and showing that the styrenes of the polymer pack against the acyl chains of the lipid. Interestingly, weak NOEs were also observed to the choline head group of DMPC of similar intensity to that of the acyl terminal methyl (*M*), suggesting that the styrene group intercalates across the length of the acyl chain, including both ends of the inserted DMPC molecule. Of note, weak NOEs were observed from the methylene groups of DMPC to its headgroup in the d54-form of DMPC suggesting incomplete deuteration of the lipid acyl chains. This was later confirmed by 1D analysis of

d-54 DMPC (Fig. S1 in the Electronic Supplementary Material (ESM)).

3.5 Differential scanning calorimetry

Results from SANS, NMR and polarized infrared spectroscopy suggest an intimate contact between the SMA and the lipid bilayer in SMALP particles. The polarized IR data indicates both that the styrene moiety is oriented in such a manner to suggest that it may intercalate between the acyl chains of the lipids. In addition, the signals for the acyl chains suggest that the presence of the SMA may induce some lipids to change their conformation. To assess whether the SMA has indeed disrupted the phase transition behavior of DMPC, DSC experiments were carried out on DMPC SMALPs (the SMA alone showed no transition, Fig. S2 (in the ESM)) and the results compared to those for DMPC vesicles. DSC data from free DMPC bilayers (Fig. 13, *left*) shows the presence of a clear transition at 24 ˚C which represents gel to liquid phase transition alongside a smaller transition around 13 ˚C. These observations agree well with those measured for DMPC in the past [30, 31]. Examination of the DSC data for the DMPC bilayer incorporated into the SMALP show clear perturbation of the gel to liquid transition behavior (Fig. 13 *right*). In the SMALP the gel to liquid transition broadens significantly and the transitions temperature decreases marginally to 23 ˚C. A similar broadening of the gel–liquid transition has been observed for other lipid disc encapsulations systems. These have included studies of lipid discs stabilized by membrane stabilizing peptides (MSP) [9] and those stabilized by 3:1 SMA polymer [12]. In the MSP study a similar broadening of the liquid to gel phase transition is observed while the transition temperature of the MSP stabilized discs in this case increased to 28 ˚C. This change in behavior of the lipid phase transition is explained by Shaw et al. [9] as resulting from a loss of cooperativity within the phase transition, perhaps resulting from the presence of a boundary of non-melting lipids on the interface with the polymer. For the 3:1 SMA polymer stabilized discs a lowering of the transition temperature of DMPC in SMALPs was also recorded. We interpret our data in the same way considering

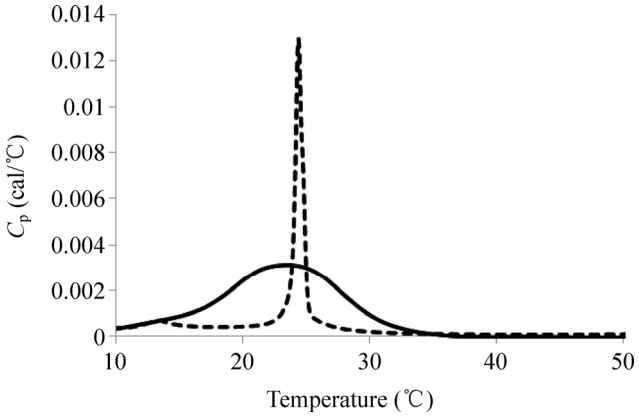

Figure 13 DSC data for DMPC vesicles (dotted line) showing two transitions at 14 ˚C and 24 ˚C and of the SMALP (solid line) showing a broadening of the gel to liquid transition (23 ˚C).

the identification of close interactions between the polymer and the lipid identified in previous sections. These interactions are likely to alter the dynamics of the lipids immediately adjacent to the polymer annulus thereby reducing the cooperative nature of the phase transition. Interestingly the studies of MSP noted that repeated scanning of the sample in the DSC (which involves repeated heating of the sample to 90 ˚C) led to a re-appearance of the sharp transition observed for the non-encapsulated lipid [9]. The appearance of this transition could indicate that the structural integrity of the disc has been disrupted by elevated temperature leading to the formation of lipid only aggregates. To test whether a similar effect could occur with the SMALP system we carried out a similar experiment by repeatedly scanning the DSC instrument 35 times from 5 to 90 ˚C (data not shown). These data showed no such return of the sharp transition. This indicates that, unlike the MSPs, the structural integrity of the SMALPs is resistant to elevated temperature. We note that that unlike our observations with the 2:1 SMA polymer, Orwick et al. [12] observed a lowering of the transition temperature of DMPC in SMALPs made using 3:1 SMA.

4 Discussion and conclusions

The membrane protein extraction method based on styrene maleic acid co-polymer [11] resolved one of the major limitations encountered with other nano-encapsulation methods. The SMALP method does not

require a detergent to extract the membrane protein from the biological membrane before its reinsertion into the membrane nanoparticle and can be used to understand the structure and function of membrane proteins. However before these studies can be undertaken the physical characteristics of the SMALP have to be determined in order to optimize and engineer their properties and capabilities.

In this study we present a more detailed structure of the SMALP (Fig. 14). These results show that the structure of SMALPs produced from DMPC bilayer is formed by SMA encircling the edge of the membrane disc. The study also shows that the geometric structure of the membrane within the disc is maintained. This is essential if the isolated membrane is going to provide an environment that mimics the native membrane lamella. Analysis of the size distribution of the disc showed a bimodal distribution of diameters centered on ~11 and ~16 nm. These results can be compared with a similar electron microscopy study of SMALPs made using the 3:1 polymer which showed that the diameter of the particles varied between 5–15 nm [12]. Our observation of bimodality may also indicate something about how the polymer interacts with the bilayer during formation. For example it may mean that there are discrete numbers of lipids that can be stabilized by the SMA to form a viable disc with excess material potentially being accumulated in larger aggregates. Optimizing this balance in future studies could be of importance in increasing yields of discs from membranes.

The dimensions of the SMALP defined by the SANS experiments provides a clear picture of the partition of space in the particle between the polymer and lipid. These data also allow an estimation of the number of lipids that are encapsulated within the particle. If it is assumed that the area of each DMPC molecule within the bilayer is 59.6 Å^2 [23] then each leaflet of the bilayer within the SMALP contains approximately 70 DMPC molecules or 140 in the bilayer. This value is similar to figures calculated for the MSP stabilized lipid discs developed by Sligar and colleagues [9]. These data also allow us to estimate the size of a membrane protein that can be included in a SMALP. From the SANS data we can assume a maximum radius for the membrane in the SMALP of 40 Å. The radius of an α-helix can vary depending upon on side chain identity and conformation. In transmembrane helices the three most abundant side chains are the hydrophobic amino acids leucine, isoleucine and valine.

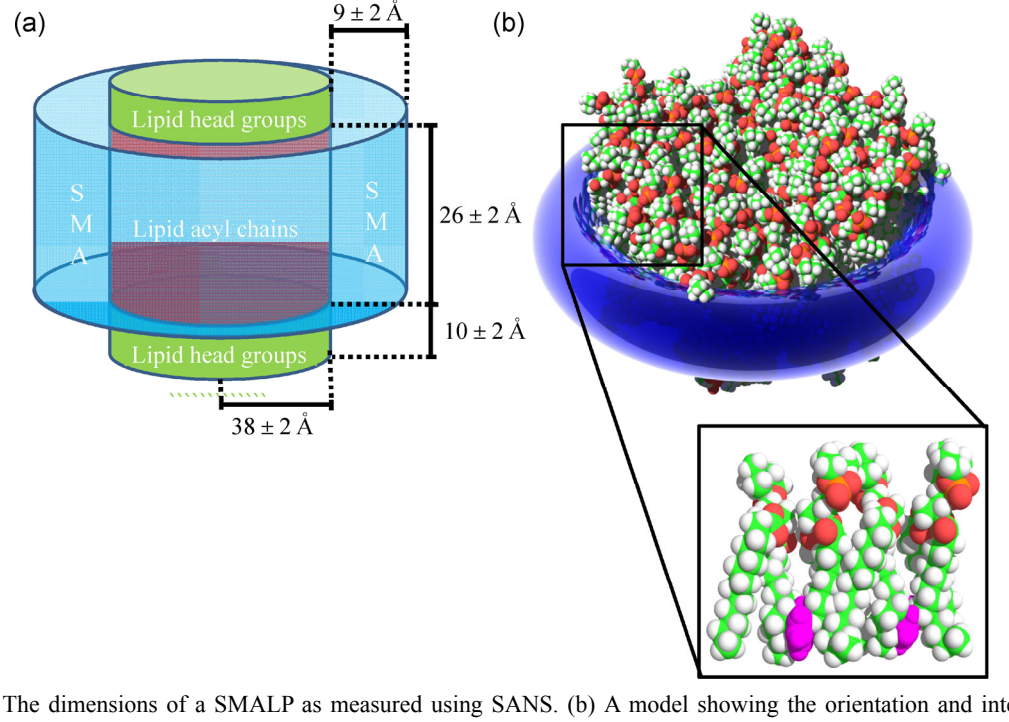

Figure 14 (a) The dimensions of a SMALP as measured using SANS. (b) A model showing the orientation and interactions of the benzene moieties (purple) within SMALPs.

Structural analysis of helices containing these residues provides an average diameter for the helix of approximately 12 Å. Once the diameters of the two species (the SMALP and α-helix in this case) are defined, then the packing of one into the other becomes a problem of packing circles in circles. If perfect packing (e.g., with no wasted space between packed objects) could be achieved, then the packing density is the quotient of the areas of the two circles which is 40. This represents an unlikely upper limit of packing as rigid circles do not pack against each other perfectly (unlike hexagons). For rigid circles the maximum packing density of circles on a flat plane is approximately 0.91 (proved by LászlóFejes-Tóth in 1940 [32]) meaning that 36 helices could pack into a SMALP. However when applied to the problem of packing circles within circles this number is reduced further as the shape of the outer boundary further restricts the packing to 34 helices [33]. In the case of packing helices in the SMALP it also has to be considered that this packing problem is not necessarily described perfectly by the packing of rigid circles inside a rigid circle. It is possible that α-helixes could achieve higher levels of packing than rigid circles as inter-helical side chains can intercalate with one another producing what is in effect a packing of deformable circles. We can therefore only say that the packing density of α-helices in the SMALP with these dimensions is not likely to exceed 40 α-helices per SMALP but could exceed the theoretical maximum of 34 for packing of rigid circles of 6 Å radius in a circle with radius of 40 Å.

Both SANS and ATR-FTIR measurements suggest that the SMA polymer takes the form of a "bracelet" encircling the lipid membrane with the styrene moieties oriented parallel to the membrane normal. NMR confirms that the styrene moieties interact directly with the acyl chains of the lipids and it is most likely that they intercalate approximately midway along the acyl chains. Our data also shows that the maleic acid groups are oriented in the same direction as the styrene moieties but are likely to interact with the lipid headgroups confirming the work of Orwick et al. [12].These data suggest that one of the major driving forces for the spontaneous formation of the SMALPs is likely to be the burial of the styrene groups into the hydrophobic core of the membrane.

The picture of interactions between the polymer and lipid could lead to an alteration in the membrane fluidity disrupting its ability to mimic a conventional membrane bilayer continuum. To examine this we carried out a study of the membrane phase transitions using DSC. These data indicate that like other disc systems the main phase transition is broadened indicating a loss of cooperativity. This is likely to be produced by the interactions between the lipids and the polymer. We also observe a perturbation of the transition temperature by 1 °C. This contrasts with calorimetry data reported by Orwick et al. [12] which indicated that the 3:1 SMA caused the transition temperature to reduce considerably (by approximately 10 °C) while a study of the MSP system reported an increase in transition temperature of 3 °C. These changes in transition temperature further indicate a perturbation of the lipid bilayer. The lowering of the transition temperature in the SMA 3:1 discs is significant and could be of some concern if membrane fluidity is important in the conformational flexibility of any proteins contained in the encapsulated membrane. This is particularly important for proteins where a conformational change is important for function (i.e., G protein coupled receptors). Our DSC study also indicates that the structure of the SMALP is resistant to repeated exposure to elevated temperatures when compared to the MSP system. This observation suggests that the SMA systems may provide a more resilient encapsulation method compared to that offered by the MSP. Interestingly, the differences observed between the two SMA polymers so far studied offers the intriguing possibility that other formulations of the SMA polymer may provide SMALPs with different physical characteristics. It is therefore important that further studies are carried out to assess other SMA polymers with different molecular weights and compositions that may offer an improved solution to this important problem.

Taken together our study provides useful information on the structure of the SMALP for those planning on using nanoparticle systems to study proteins and membranes, and highlights the distinguishing properties that offer advantages for native state solubilization and characterization.

Acknowledgements

TD, MO, MJ, ORTT, TK, NS, MW, YPL, RF, and KJE would like to acknowledge the support of the Biotechnology and Biological Sciences Research Council (BBSRC) through grants BB/G010412/1, BB/I020349/1, BB/I019960/1, BB/I013865 and BB/J017310/1 and Follow on Funding. NMR data were collected at Henry Wellcome Building, a national NMR facility (HWB-NMR) which is supported by the Wellcome Trust. VG and CG were supported by the F.R.S.–Fonds de la Recherche Scientifique (FNRS). KJE and II acknowledge the ILL for provision of beam time on D11 (experiment 9-13-344) and the assistance of Dr. Ralf Schweins in collecting and reducing the SANS data. II acknowledges the Science & Technology Facilities Council (STFC) BioMemembrane Network (No. BMN10-01) and the University of Bath for funding. We thank Erik Goormaghtigh for discussions about interpretation of the IR data and Christian Ludwig for his help in setting up the NMR experiments. We thank Cameron Neylon for discussions about interpretation of the SANS data. We also thank Malvern Cosmeceutics Ltd. for initial discussions about the production of SMALPs.

Electronic Supplementary Material: Supplementary material (NMR spectra and differential scanning calorimetry data) are available in the online version of this article at http://dx.doi.org/10.1007/s12274-014-0560-6.

References

[1] Lin, S. H.; Guidotti, G. Purification of membrane proteins. *Methods Enzymol.* **2009**, *463*, 619–629.

[2] Lichtenberg, D.; Ahyayauch, H.; Alonso, A.; Goñi, F. M. Detergent solubilization of lipid bilayers: A balance of driving forces. *Trends Biochem. Sci.* **2013**, *38*, 85–93.

[3] Bayburt, T. H.; Carlson, J. W.; Sligar, S. G. Reconstitution and imaging of a membrane protein in a nanometer-size phospholipid bilayer. *J. Struct. Biol.* **1998**, *123*, 37–44.

[4] Borch, J.; Torta, F.; Sligar, S. G.; Roepstorff. P. Nanodiscs for immobilization of lipid bilayers and membrane receptors: Kinetic analysis of cholera toxin binding to a glycolipid receptor. *Anal. Chem.* **2008**, *80*, 6245–6252.

[5] Bayburt, T. H.; Sligar, S. G. Membrane protein assembly into nanodiscs. *FEBS Lett.* **2010**, *584*, 1721–1727.

[6] Denisov, I. G.; Grinkova, Y. V.; Baas, B. J.; Sligar, S. G. The ferrous-dioxygen intermediate in human cytochrome P450 3A4. Substrate dependence of formation and decay kinetics. *J. Biol. Chem.* **2006**, *281*, 23313–23318.

[7] Leitz, A. J.; Bayburt, T. H.; Barnakov, A. N.; Springer, B. A.; Sligar, S. G. Functional reconstitution of Beta2-adrenergic receptors utilizing self-assembling nanodisc technology. *BioTechniques* **2006**, *40*, 601–612.

[8] Shaw, A. W.; Pureza, V. S.; Sligar, S. G.; Morrissey, J. H. The local phospholipid environment modulates the activation of blood clotting. *J. Biol. Chem.* **2007**, *282*, 6556–6563.

[9] Shaw, A. W.; McLean, M. A.; Sligar, S. G. Phospholipid phase transitions in homogeneous nanometer scale bilayer discs. *FEBS lett.* **2004**, *556*, 260–264.

[10] Tonge, S. R.; Tighe, B. J. Responsive hydrophobically associating polymers: A review of structure and properties. *Adv. Drug Deliver. Rev.* **2001**, *53*, 109–122.

[11] Knowles, T. J.; Finka, R.; Smith, C.; Lin, Y. P.; Dafforn, T.; Overduin, M. Membrane proteins solubilized intact in lipid containing nanoparticles bounded by styrene maleic acid copolymer. *J. Am. Chem. Soc.* **2009**, *131*, 7484–7485.

[12] Orwick, M. C.; Judge, P. J.; Procek, J.; Lindholm, L.; Graziadei, A.; Engel, A.; Gröbner, G.; Watts, A. Detergent-free formation and physicochemical characterization of nanosized lipid-polymer complexes: Lipodisq. *Angew. Chem. Int. Ed.* **2012**, *124*, 4731–4735.

[13] Orwick-Rydmark, M.; Lovett, J. E.; Graziadei, A.; Lindholm, L.; Hicks, M. R.; Watts, A. Detergent-free incorporation of a seven-transmembrane receptor protein into nanosized bilayer lipodisq particles for functional and biophysical studies. *Nano lett.* **2012**, *12*, 4687–4692.

[14] Long, A. R.; O'Brien, C. C.; Malhotra, K.; Schwall, C. T.; Albert, A. D.; Watts, A.; Alder, N. N. A detergent-free strategy for the reconstitution of active enzyme complexes from native biological membranes into nanoscale discs. *BMC biotechnol.* **2013**, *13*, 41.

[15] Bechinger, B.; Ruysschaert, J. M.; Goormaghtigh, E. Membrane helix orientation from linear dichroism of infrared attenuated total reflection spectra. *Biophys. J.* **1999**, *76*, 552–563.

[16] Dalvit, C.; Ramage, P.; Hommel, U. Heteronuclear X-filter 1H PFG double-quantum experiments for the proton resonance assignment of a ligand bound to a protein. *J. Magn. Reson.* **1998**, *131*, 148–153.

[17] Hwang, T. L.; Shaka, A. J. Water suppression that works. Excitation sculpting using arbitrary wave-forms and pulsed-field gradients. *J. Magn. Reson.* **1995**, *112*, 275–279.

[18] Delaglio, F.; Grzesiek, S.; Vuister, G. W.; Zhu, G.; Pfeifer, J.; Bax, A. NMRPipe: A multidimensional spectral processing system based on UNIX pipes. *J. Bio. NMR* **1995**, *6*, 277–293.

[19] Goddard, T. D.; Kneller, D. G. SPARKY 3. *University of California, San Francisco,* **2004**, 15.

[20] Kline, S. R. Reduction and analysis of SANS and USANS data using IGOR Pro. *J. Appl. Cryst.* **2006**, *39*, 895–900.

[21] Hayter, J. B.; Penfold, J. An analytic structure factor for macroion solutions. *Mol. Phys.* **1981**, *42*, 109–118.

[22] Smith, M. B.; McGillivray, D. J.; Genzer, J.; Lösche, M.; Kilpatrick, P. K. Neutron reflectometry of supported hybrid bilayers with inserted peptide. *Soft Matter* **2010**, *6*, 862–865.

[23] Nagle, J. F.; Tristram-Nagle, S. Structure of lipid bilayers. *BBA-Rev. Biomembranes* **2000**, *1469*, 159–195.

[24] Goormaghtigh, E.; Raussens, V.; Ruysschaert, J. M. Attenuated total reflection infrared spectroscopy of proteins and lipids in biological membranes. *BBA-Rev. Biomembranes* **1999**, *1422*, 105–185.

[25] Liang, C. Y.; Krimm, S. Infrared spectra of high polymers. VI. Polystyrene. *J. Polym. Sci.* **1958**, *27*, 241–254.

[26] Raussens, V.; Narayanaswami, V.; Goormaghtigh, E.; Ryan, R. O.; Ruysschaert, J. M. Alignment of the apolipophorin-III alpha-helices in complex with dimyristoylphosphatidylcholine. A unique spatial orientation. *J. Biol. Chem.* **1995**, *270*, 12542–12547.

[27] Fringeli, U. P.; Günthard, H. H. Infrared membrane spectroscopy. *Mol. Biol. Biochem. Biophys.* **1981**, *31*, 270–332.

[28] Lewis, R. N.; Pohle, W.; McElhaney, R. N. The interfacial structure of phospholipid bilayers: Differential scanning calorimetry and Fourier transform infrared spectroscopic studies of 1,2-dipalmitoyl-*sn*-glycero-3-phosphorylcholine and its dialkyl and acyl-alkyl analogs. *Biophys. J.* **1996**, *70*, 2736–2746.

[29] Wald, J. H.; Coormaghtigh, E.; Meutter, J. D.; Tuysschaert, J. M.; Jonas, A. Investigation of the lipid domains and apolipoprotein orientation in reconstituted high density lipoproteins by fluorescence and IR methods. *J. Biol. Chem.* **1990**, *265*, 20044–20050.

[30] Heimburg, T. A model for the lipid pretransition: Coupling of ripple formation with the chain-melting transition. *Biophys. J.* **2000**, *78*, 1154–1165.

[31] Blume, A. Apparent molar heat capacities of phospholipids in aqueous dispersion. Effects of chain length and head group structure. *Biochem.* **1983**, *22*, 5436–5442.

[32] Fejes Tóth, L. *Regular Figures*; Pergamon Press: Oxford, 1964; pp 339.

[33] Specht, E. *program cci*, 1999–2014.